# InP Photonic Integrated Circuit for 6.7GHz Spaced Optical Frequency Comb Generator

Euan J. Tough*, Martyn J. Fice, Cyril C. Renaud, James Seddon, Alwyn J. Seeds, Chris Graham, Katarzyna Balakier
*Department of Electronic and Electrical Engineering*
*University College London*
London, UK
*uceetou@ucl.ac.uk

Guillermo Carpintero
*Department of Electronic Technology*
*Universidad Carlos III de Mardrid,*
Madrid, Spain
ORCID # 0000-0001-6665-3977

2021 International Topical Meeting on Microwave Photonics (MWP) | 978-1-6654-2610-7/21/$31.00 ©2021 IEEE | DOI: 10.1109/MWP53341.2021.9639427

***Abstract*—We have demonstrated a novel approach to photonically integrated optical frequency comb generation on Indium Phosphide (InP) using generic foundry platforms. The optical comb utilized a recirculating loop technique to generate 59 comb lines (within a 20 dB power envelope) which are separated by 6.7 GHz frequency spacing. All comb lines exhibit strong phase coherence as characterized by low phase noise measurements of -105 dBc/Hz at 100 kHz. The choice of InP as an integration platform allowed for an immediate optical amplification of the modulated sideband tones. This approach reduced the requirement for external high-power RF amplifiers and therefore made the entire system more compact and power efficient. The amplified recirculating loop comb occupied 6 x 0.7 mm$^2$ area of InP chip and consisted of electro-optic phase modulator (EOPM) and semiconductor optical amplifier (SOA) components embedded within a short (12 mm long) waveguide loop, such that the round-trip loop frequency corresponding to the loop optical length equated to 6.7 GHz. Modulation frequencies equal to the round-trip loop frequency were used to generate broad comb spans.**

***Keywords—photonic integrated circuits, optical frequency combs***

## I. Introduction

Optical frequency comb generators (OFCGs) are optical sources capable of generating multiple phase coherent optical tones evenly spaced across broad optical bandwidths and are a fundamental component in many microwave photonic systems. Applications that have benefited from comb generation span many disciplines including spectroscopy [1], LIDAR [2], THz generation [3], high-speed optical communications [4] and RF over fibre [5]. The required properties for an OFCG are often driven by the application which has resulted in numerous OFCG techniques to be developed. Generally, OFCG techniques based on bulk components have provided sufficient diversity in comb properties to accommodate the expansive range of applications, however their size, weight and power consumption (SWaP) can present difficulties for practical implementations. To this end significant research efforts has been directed towards making the OFCG smaller and more portable.

Recently, an effort to translate OFCG systems to monolithically integrated devices has been enabled by advances in fabrication techniques and the increased availability of generic foundry platforms. Photonic integrated circuits (PICs) can support a high density of active and passive components enabling the miniaturization of complex optical systems into compact integrated packages that typically exhibit reduced optical losses and power consumption demands. Integrated OFCGs have been demonstrated in various configurations including mode-locked lasers [6], Kerr-comb micro-resonators [7], gain-switched lasers [8], and cascaded electro-optic (EO) comb generators [9].

In this work we present a novel technique of integrated EO OFCG implementing an amplified recirculating loop that has been fabricated using widely available building blocks on the InP generic foundry platform.

## II. Principle of Operation

A high-level schematic of the amplified recirculating loop technique of optical frequency comb generator which was first proposed in [10] and is presented in Fig. 1. It consists of a recirculating loop formed from an optical waveguide with a phase modulator and optical amplifier situated within it. A continuous wave reference laser injected into the loop is modulated to generate frequency shifted sidebands that are equally spaced by the applied modulation frequency. The loop enables the optical signal to be recirculated through the phase modulator multiple times such that it experiences enhanced modulation on successive passes. Optical amplification within the loop provides sufficient gain to compensate for round-trip waveguide propagation losses of the loop so that a large portion of the optical power can be distributed to higher order sidebands, allowing broad comb spans to be generated.

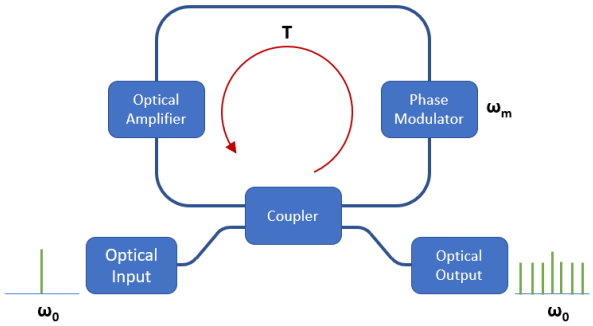


Fig. 1. Schematic of the amplified recirculating loop technique of OFCG

Optimal operation to efficiently enhance modulation on each recirculation is achieved when the design of the loop and the specification of both the optical reference and modulation drive frequencies fulfil the following conditions:

$$\omega_m T = 2p\pi \quad (1)$$

$$\omega_0 T = 2q\pi \quad (2)$$

Where T represents the round-trip time delay which is a property of the loop and is defined by its length and the group index of the optical waveguide. Condition 1 is satisfied when the phase modulator is driven by a modulation frequency ($\omega_m$) equal to an integer harmonic (p) of the round-trip time delay (T), ensuring that the frequency of the phase modulation sidebands coincide with the cavity modes supported by the loop resonance. The second condition states that the frequency of the reference laser source ($\omega_0$) coupled into the recirculating loop must similarly be tuned to an integer harmonic (q) of the round-trip time delay (T) such that the recirculating optical signal is reinforced by the injected reference source.

Previous works on this technique [11,12] have been compiled from bulk components embedded within fibre-based loops that are ~20 m in length. Though excellent performance of these systems has been demonstrated, the length of the fibre loop produces narrow round-trip loop frequencies on the order of 10's of MHz. Comb generation at GHz frequency spacing can be achieved by driving the modulator with an integer harmonic of the loop frequency as outlined in Eq. (1). However, the generated comb lines are interleaved by many closely spaced adjacent modes that encourages mode hopping behaviour. Therefore, without locking or feedback mechanisms these fibre-based systems suffer from instability and are sensitive to detuning effects of both $\omega_m$ and $\omega_0$.

Integration of the system on PIC provided the unique capability to fabricate waveguide loops with significantly shorter lengths compatible with round-trip time delays that correspond to frequency spacings of several GHz. Conceptually, the system can then be driven with modulation frequencies that are directly equal to the cavity modes of the loop rather than a harmonic, removing the existence of closely spaced adjacent modes between comb lines and thus inherently improving the stability of the comb generation without additional feedback mechanisms.

## III. Experimental Setup

### A. PIC Design

The InP PIC was fabricated as part of a multi-project wafer run using generic foundry methods, with multiple iterations of the integrated comb generator design contained within the 6 x 2 $mm^2$ PIC footprint. An image depicting the test structure and the equivalent schematic can be seen in Fig. 2a and Fig. 2b respectively.

Input and output facets on PIC were defined by vertically tapered waveguide spot-size converters (SSCs) which optimised coupling efficiency. The SSCs were angled at 7° and an anti-reflective coating was applied to the facets that minimised the effects of back-reflections. Optical inputs and outputs were coupled to the PIC through lensed fibres launched at a 22° offset to the normal, enabling effective coupling to the angled SSCs. Passive waveguides on the PIC were comprised of deep-etched waveguides with ~7 dB/cm propagation losses. A minimum bend radius of 150 µm was chosen such that negligible additional losses were contributed. Input and output waveguides were coupled to the recirculating loop by a 2x2 multimode interference (MMI) coupler with a 50:50 splitting ratio.

The loop had a total length of 12 mm and was embedded with two multiple-quantum-well (MQW) semiconductor optical amplifiers (SOAs) and two MQW electro-absorption modulators operated in reverse bias which enabled phase modulator behaviour by the quantum confined Stark effect (QCSE). The two phase modulator components were linearly cascaded within the loop so that the effective modulation index was increased by a factor of 2, enabling additional comb lines to be generated with reduced peak-to-peak voltage ($V_{pp}$) provided to each component. Furthermore, a short phase shifter (PS) section was included inside the loop capable of tuning the refractive index over a small range by direct current injection.

The InP PIC was mounted to an aluminium nitride subassembly alongside Alumina interposers with thermally and electrically conductive epoxy. Electrical connections

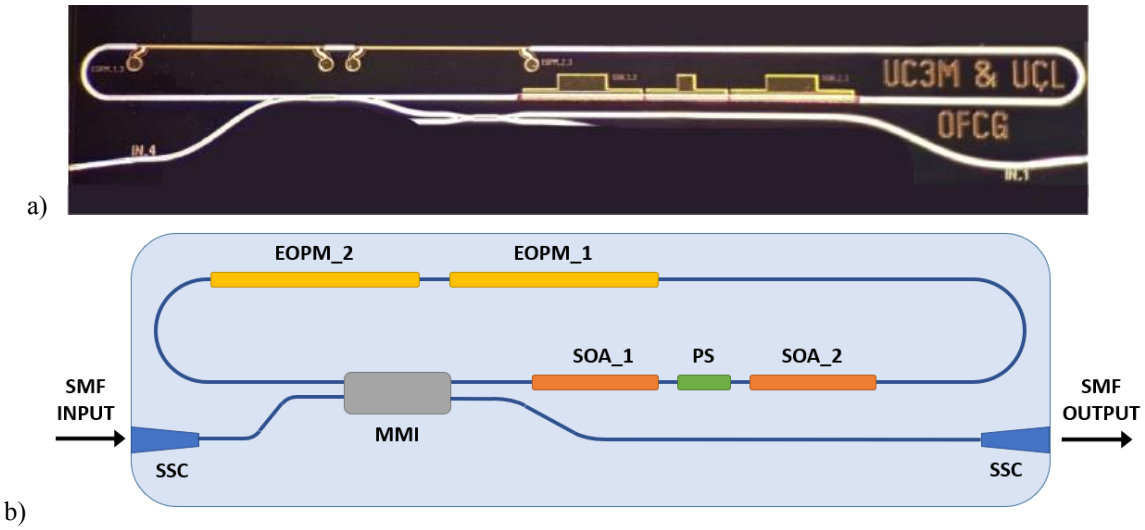


Fig. 2. (a) An image of the amplified recirculating loop on PIC. (b) Schematic depicting the components of the integrated amplified recirculating loop device

were made by wire bonding between the gold contacts on the PIC and the patterned gold surfaces of the interposer which contained a combination of grounded coplanar transmission lines with ground-signal-ground dimensions designed to operate at 50 Ω impedance, and DC signal lines. The RF connections were then extended with wire bonds from the interposer to a pitch increasing custom printed circuit board (PCB) with multiple soldered SMA RF port connectors. Each electro-optic phase modulator was connected to two RF ports where one was used to provide the biased RF drive signal whilst the other was terminated at 50 Ω. DC pin probes were used to inject current to each of the SOAs and PS sections directly via the interposer. The subassembly was mounted using the same conductive epoxy to a copper heatsink block which was grounded and thermally stabilised at 20 °C by a thermo-electric cooler (TEC).

### B. *Comb Generation*

Comb generation was performed by injecting an optical input supplied by a tuneable external cavity laser source with a linewidth of 100 KHz and power set at 10 dBm to avoid gain saturation of the SOA components. The wavelength was set to 1550 nm then tuned to the nearest integer harmonic of the round-trip loop frequency.

The modulation frequency was set directly equal to the measured round-trip loop frequency of 6.71 GHz and supplied by an externally referenced R&S SMF100A signal generator outputting 15 dBm power. The signal was split by an appropriate bandwidth RF splitter to allow synchronous modulation to each of the EOPMs via RF phase shifter delay lines that provided precise control of the phase alignment to phase match the electrical drives supplied to the EOPMs. Once losses in the splitter and phase shifters were accounted for, it was necessary to amplify the RF signal with low noise RF amplifiers that boosted the power to around 24 dBm ($V_{pp}$ ~10 V) per channel. Each amplified RF signal was provided with a reverse bias of -7 V via bias tee components for optimal operation of the phase modulators and was then delivered to ports on the PCB corresponding to the EOPMs on PIC.

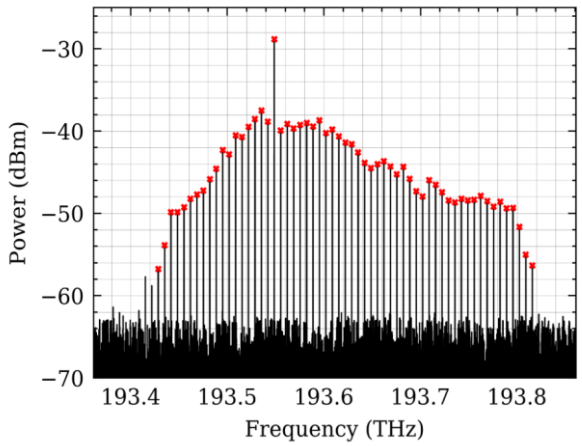


Fig. 4. Optical spectrum generated by the amplified recirculating loop technique with resolution bandwidth of 10 MHz. Red crosses identify peaks contained within a 20 dB power envelope that excludes the carrier frequency

Table 1

| FSR | Number of Comb Line within Power Envelope | | | |
|---|---|---|---|---|
| | *3 dB* | *5 dB* | *10 dB* | *20 dB* |
| 6.71 GHz | 14 | 20 | 37 | 59 |

SOA and PS sections were controlled by a Thorlabs PRO8000 current control rack via independently driven pin probes in direct contact with the DC signal lines on the interposer sub-assembly. SOA_1 was driven at transparency with around 12.5 mA, whilst SOA_2 was driven at around 65 mA so that sufficient gain was provided to compensate for the loop losses. The PS section was driven with small injection currents of <1.0 mA and used to perform finely tuned optimisation of the loop length.

Optimization of the comb was performed through fine adjustment of the electrical and optical phase shifters, and polarization controller whilst monitoring the comb output on an Aragon Photonics BOSA 400 high-resolution (0.08 pm) optical spectrum analyzer. Maximum comb spans were observed when both the carrier frequency and the modulation frequency corresponded to the resonant conditions of the loop. Phase noise measurements were recorded from the electrical response of the comb on a high-speed photodiode measured on an R&S FSU Spectrum Analyzer.

## IV. Results and Discussion

The generated comb can be seen in Fig. 4 outputting 59 comb lines equally spaced by the modulation frequency of 6.71 GHz and spanning approximately 395 GHz within a 20 dB power envelope. An average of 20 dB per comb line was observed as a result of compensation of losses in the loop by the embedded optical amplification. The carrier frequency presented the strongest peak power with a ~10 dB power discrepancy when compared to the adjacent sidebands and

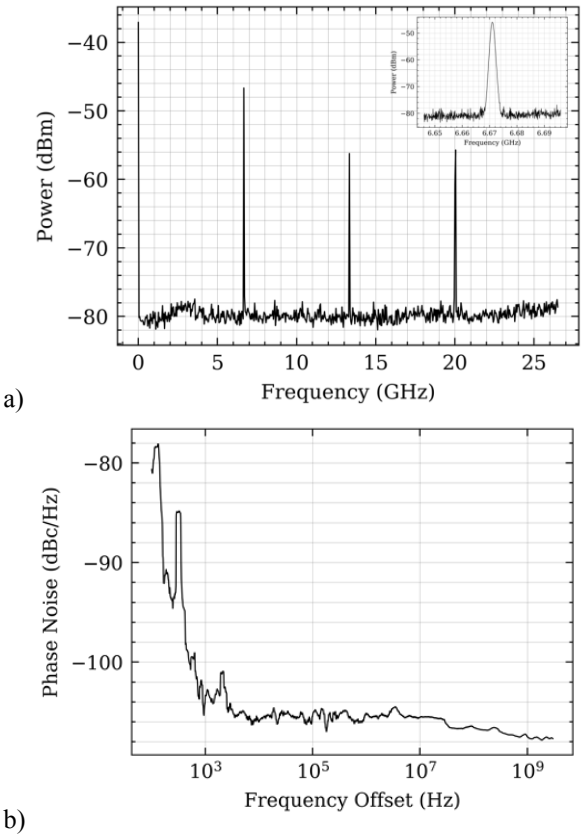


Fig. 5. (a) The electrical spectrum of the comb with a resolution bandwidth of 1 MHz as measured on a high-speed photodiode demonstrating defined peaks at multiples of the FSR The inset shows a close-up of the first peak (b) the phase noise measured for the first peak

was an outcome of the 50% splitting ratio of the MMI enabling half of the optical input to propagate through the PIC without entering the loop. Flatness of the comb drops off with reduced power envelopes as summarised in Table. 1.

The electrical spectrum in Fig. 5a demonstrates strong and distinct peaks at integer harmonics of the round-trip loop frequency and applied modulation frequency. Only 3 peaks are shown due to a limitation in bandwidth of the measurement equipment. The inset in Fig. 5a depicts a zoomed perspective of the electrical response of the photodiode for the 6.71 GHz peak covering a span of 50 MHz with a resolution bandwidth of 1 MHz. The narrow peak indicates good phase coherence which is further demonstrated by the phase noise measurement of -105 dBc/Hz at 100 kHz shown in Fig. 5b.

## V. Conclusions

In this paper we demonstrated the first monolithically integrated realization of the amplified recirculating loop technique of OFCG. The compact device generated broad optical combs through successive passes of EOPMs in the loop and demonstrates good comb line power. By operating with modulation frequencies directly equal to the round-trip loop frequency the integrated loop design encouraged strong phase coherence between comb lines as demonstrated by low phase noise characteristics.

## Acknowledgments

This research work has been supported by the UK Engineering and Physical Sciences Research Council through the Integrated Photonics and Electronic Systems (IPES) Centre of Doctoral Training and PICSat (EPSRC Reference: EP/S000976/1).

## References

[1] H. Song *et al.*, "Broadband-frequency-tunable sub-terahertz wave generation using an optical comb, AWGs, optical switches, and a uni-traveling carrier photodiode for spectroscopic applications," Journal of Lightwave Technology, vol. 26, no. 15, pp. 2521-2530, Aug.1, 2008.

[2] T. Fortier, E. Baumann, "20 years of developments in optical frequency comb technology and applications," *Commun Phys 2*, 153, 2019.

[3] T. Tetsumoto *et al.*, "Optically referenced 300 GHz millimetre-wave oscillator*," Nat. Photon*. 15, 516–522, 2021.

[4] H. Hu, and L. Oxenløwe, "Chip-based optical frequency combs for high-capacity optical communications," *Nanophotonics*, vol. 10, no. 5, pp. 1367-1385, 2021.

[5] M. Piccardo, *et al.*, "Radio frequency transmiter based on laser frequency comb," *PNAS,* vol. 116, no. 19, pp. 9181-9185, 2019.

[6] K. Van Gasse *et al*., "Recent advances in the photonic integration of mode-locked laser diodes," *IEEE Photonics Technology Letters*, vol. 31, no. 23, pp. 1870-1873, 1 Dec.1, 2019

[7] B. Stern, X. Ji, Y. Okawachi, A.L. Gaeta, and M. Lipson, "Battery-operated integrated frequency comb generator," *Nature*, 562, 401–405, 2018.

[8] M. D. G. Pascual *et al*., "Photonic integrated gain switched optical frequency comb for spectrally efficient optical transmission systems," *IEEE Photonics Journal*, vol. 9, no. 3, pp. 1-8, June 2017.

[9] F. Bontempi, N. Andriolli, F. Scotti, M. Chiesa, and G. Contestabile, "Comb line multiplication in an integrated optical frequency comb generator," *2019 24th OptoElectronics and Communications Conference (OECC)*, pp. 1-3, 2019.

[10] K. Ho and J. M. Kahn, "Optical frequency comb generator using phase modulation in amplified circulating loop," *IEEE Photonics Technology Letters*, vol. 5, no. 6, pp. 721-725, June 1993.

[11] S. Bennett, B. Cai, E. Burr, O. Gough, and A. J. Seeds, "1.8-THz bandwidth, zero-frequency error, tunable optical comb generator for DWDM applications," *IEEE Photonics Technology Letters*, vol. 11, no. 5, pp. 551-553, May 1999

[12] L. Ponnampalam, M. Fice, H. Shams, C. Renaud, and A. Seeds, "Optical comb for generation of a continuously tunable coherent THz signal from 122.5 GHz to >2.7 THz," *Opt. Lett*. vol. 43, no. 11, pp. 2507-2510,